Nucleoside Diphosphate Kinase from Bovine Retina: Purification, Subcellular Localization, Molecular Cloning, and Three-Dimensional Structure†

Najmoutin G. Abdulaev,‡,§ Galina N. Karaschuk,§ Jane E. Ladner,‡ Dmitri L. Kakuev,§ Alexei V. Yakhyaev,§ Maria Tordova,‡ Ibragim O. Gaidarov,§ Viktor I. Popov,|| John H. Fujiwara,‡ Diana Chinchilla,‡ Edward Eisenstein,‡ Gary L. Gilliland,‡ and Kevin D. Ridge*,‡

Center for Advanced Research in Biotechnology, National Institute of Standards and Technology and the University of Maryland Biotechnology Institute, 9600 Gudelsky Drive, Rockville, Maryland 20850, The Laboratory of Light Sensitive Systems, Shemyakin and Ovchinnikov Institute of Bioorganic Chemistry, Russian Academy of Sciences, Moscow, Russia, and the Institute of Biological Physics, Russian Academy of Sciences, Pushchino, Moscow Region, Russia

Received April 15, 1998; Revised Manuscript Received July 30, 1998

ABSTRACT: The biochemical and structural properties of bovine retinal nucleoside diphosphate kinase were investigated. The enzyme showed two polypeptides of ∼17.5 and 18.5 kDa on SDS−PAGE, while isoelectric focusing revealed seven to eight proteins with a pI range of 7.4−8.2. Sedimentation equilibrium yielded a molecular mass of 96 ± 2 kDa for the enzyme. Carbohydrate analysis revealed that both polypeptides contained Gal, Man, GlcNAc, Fuc, and GalNac saccharides. Like other nucleoside diphosphate kinases, the retinal enzyme showed substantial differences in the K_m values for various di- and triphosphate nucleotides. Immunogold labeling of bovine retina revealed that the enzyme is localized on both the membranes and in the cytoplasm. Screening of a retinal cDNA library yielded full-length clones encoding two distinct isoforms (NBR-A and NBR-B). Both isoforms were overexpressed in *Escherichia coli* and their biochemical properties compared with retinal NDP-kinase. The structures of NBR-A and NBR-B were determined by X-ray crystallography in the presence of guanine nucleotide(s). Both isoforms are hexameric, and the fold of the monomer is similar to other nucleoside diphosphate kinase structures. The NBR-A active site contained both a cGMP and a GDP molecule each bound at half occupancy while the NBR-B active site contained only cGMP.

Signal transduction in vertebrate photoreceptor cells begins with absorption of light by the visual pigment rhodopsin and culminates in the closure of ion channels on the plasma membrane. Consecutive binding and hydrolysis of several guanine nucleotides support the flow of information between these two events. In fact, light absorption by rhodopsin induces a GDP−GTP exchange on the heterotrimeric guanine nucleotide-binding protein (G-protein).[1] Entry of GTP into the nucleotide-binding site of the G-protein results in dissociation of the latter from the light-activated rhodopsin and separation of the $\beta\gamma$-subunit complex from the catalytic α-subunit. This, in turn, activates the downstream effector cyclic GMP phosphodiesterase (PDE) by sequestering the inhibitory constraint imposed by the PDE γ-subunit. The activated PDE hydrolyzes cGMP into 5′-GMP, and this modifies the channel function. Hydrolysis of bound GTP by the intrinsic GTPase activity of the catalytic α-subunit terminates its interaction with the effector with subsequent formation of an inactive G-protein. Synthesis of cGMP is accomplished by the membrane-bound guanylate cyclase, returning the concentration of this second messenger to its original level, thereby allowing the channel to reopen and the cell to recover (*1*−*3*).

The high levels of GTP required for G-protein activation and cGMP synthesis in the retina are likely to be supported by nucleoside diphosphate kinase (NDP-kinase). The activity of the enzyme has been measured in retinal layers and outer segments (*4*, *5*), but the enzyme itself has not been biochemically and structurally characterized. NDP-kinase presumably constitutes an integral part of the cGMP cycle (cGMP → 5′-GMP → GDP → GTP → cGMP) and catalyzes the phosphorylation of nucleoside diphosphates to nucleoside triphosphates by a Ping-Pong mechanism involving a high-energy phosphorylated enzyme intermediate. The high-energy phosphate is usually supplied by ATP (*6*).

Several mammalian, bacterial, and plant NDP-kinases have been purified and sequenced (*7*). The polypeptides range in molecular mass from 17 to 20 kDa, and in some species, two distinct soluble NDP-kinases sharing very high sequence homology have been found. Interestingly, each of these forms has different isoelectric points and mobilities on SDS−PAGE. The three-dimensional structures of several NDP-kinases are also known and the catalytic mechanisms have been studied in detail (*8*−*12*). NDP-kinases, long considered as housekeeping enzymes, are now implicated in the regula-

† This work was supported by the International Science Foundation and the National Institute of Standards and Technology (NIST).

* To whom correspondence should be addressed. Phone: 301-738-6218. Fax: 301-738-6255. E-mail: ridge@indigo2.carb.nist.gov.

‡ Center for Advanced Research in Biotechnology.

§ Shemyakin and Ovchinnikov Institute of Bioorganic Chemistry.

|| Institute of Biological Physics.

[1] Abbreviations: G-protein, guanine nucleotide-binding protein; NDP-kinase, nucleoside diphosphate kinase; PDE, phosophodiesterase; ROS, rod outer segment; RIS, rod inner segment; PAGE, polyacrylamide gel electrophoresis; PBS, phosphate-buffered saline.

S0006-2960(98)00853-8 CCC: $15.00
Published on Web 09/19/1998

tion of several fundamental cellular processes such as development (*13*), transcriptional activation (*14*), inhibition of cell differentiation (*15*), and apoptosis (*16*). In human tumors, a reduction in nm23 gene expression, an NDP-kinase family member, has been associated with increased metastatic potential of a variety of carcinomas (*7*). Interestingly, none of these functions involve their NDP-kinase activity. NDP-kinase has also been shown to function as a protein kinase that phosphorylates a serine on histone or casein and a histidine on ATP-citrate lyase (*17, 18*). More recently, NDP-kinase was shown to participate in muscarinic K^+ channel opening (*19*).

Although the key role of guanine nucleotides in visual transduction is firmly established, what remains unclear is how the phototransduction cascade blends with the biochemical pathways of nucleotide metabolism. Our previous efforts along this line have focused on guanylate kinase (*20*) and guanylate cyclase (*21*). In this paper, we have undertaken a systematic study of the biochemical and structural properties of bovine retinal NDP-kinase. The molecular properties of the enzyme, its subcellular localization, cDNA cloning, and heterologous expression, as well as three-dimensional structure, are reported.

EXPERIMENTAL PROCEDURES

Materials. Nucleotides, pyruvate kinase, lactate dehydrogenase, and phosphoenolpyruvate were from Sigma.[2] Restriction endonucleases and horseradish peroxidase conjugated goat anti-rabbit IgG were from Boehringer Mannheim, and the expression vector pALTER-*Ex*2 was from Promega. The pBluescript M13 vector was from Stratagene, and DNA purification kits were from Qiagen. Sequenase (version 2.0) and the enhanced chemiluminescence detection system were from Amersham. LR gold resin was from Polysciences (Warrington, PA), and the Ultrasphere ODS column was from Beckman. Blue Sepharose CL-6B was from Pharmacia Biotech, and crystallization screening kits were from Hampton Research. Frozen bovine retinas were from W. L. Lawson Co. (Lincoln, NE).

Purification of NDP-Kinase from Bovine Retina. The first stage of the NDP-kinase purification procedure represents a modified guanylate kinase isolation procedure from Hall and Kuhn (*5*). One hundred frozen bovine retina were thawed and suspended in 170 mL of 10 mM (Na, K, and H) PO_4, pH 7.6, containing 0.2 mM $MgCl_2$, 0.2 mM EGTA, 0.2 mM phenylmethanesulfonyl fluoride, and 0.02% NaN_3. After stirring for 30 min at 4 °C in the light, the concentrations of NaCl and $MgCl_2$ were adjusted to 150 and 4 mM, respectively. The suspension was stirred for another 30 min at 4 °C and the insoluble material was removed by centrifugation at 30000*g* for 1 h. The supernatant was centrifuged again at 100000*g* for 30 min to remove trace amounts of membranes. An equal volume of $(NH_4)_2SO_4$ solution saturated at 60 °C was added to the supernatant and stirred for 2 h at 4 °C. The precipitate was removed by centrifugation at 40000*g* for 40 min, and the supernatant was brought to 75% saturation with $(NH_4)_2SO_4$. After stirring overnight at 4 °C, the solution was centrifuged, and the pellet, which contains NDP-kinase, was resuspended in 10 mM Tris-HCl, pH 7.3, 2 mM $MgCl_2$, 0.1 mM EDTA, 1 mM DTT, and 300 mM NaCl (TMED buffer). Any insoluble material was removed by centrifugation at 100000*g* for 30 min. The clear supernatant was applied to a Blue Sepharose CL-6B column (15 × 1.5 cm) equilibrated with TMED buffer. The column was extensively washed with TMED, and NDP-kinase was eluted with TMED containing 2 mM GTP.

Spectrophotometric Assay of NDP-Kinase. NDP-kinase was assayed using a coupled pyruvate kinase−lactate dehydrogenase enzyme system as described (*22*). Briefly, the assays were done in a 1 mL reaction mixture containing 50 mM Tris-HCl, pH 7.6, 5 mM $MgCl_2$, 0.05 mM KCl, 0.1 mM phosphoenolpyruvate, 0.5 mM ATP, 0.1 mM TDP, 0.1 mg/mL NADH, 2 units of pyruvate kinase, and 2.5 units of lactate dehydrogenase. The reaction was initiated by addition of 0.5−5 μg of NDP-kinase at 25 °C. Monitoring the decrease in absorbance at 334 nm followed the oxidation of NADH, which reflects ADP formation by NDP-kinase. The specific activity of one unit of enzyme is defined as the turnover of 1 μmol of substrate in 1 min/mg of protein. To measure the apparent Michaelis constant (K_m) for the diphosphate nucleotides CDP and TDP, a constant ATP concentration equal to 2 mM was used. For determination of the K_m for the triphosphate nucleotides GTP and ATP, 1.4 mM CDP was used as the fixed substrate. The K_m values were estimated from double-reciprocal plots by the method of Florini and Vestling (*23*).

Equilibrium Sedimentation. Equilibrium sedimentation was performed with a Beckman XLA analytical ultracentrifuge using a four-hole An60-Ti rotor at 20 °C. Data were collected at 280 nm after attaining equilibrium, usually between 18 and 20 h, as an average of 25 measurements at each radial position with a nominal spacing of 0.001 cm between radial positions. The molecular weight of NDP-kinase was calculated from the analysis of the concentration distribution of the samples at sedimentation equilibrium using a partial specific volume of 0.73 mL/g as determined from the amino acid compositions. The data obtained at rotor speeds of 14 000 and 17 000 rpm were analyzed in terms of a single, homogeneous species according to

$$C_r = B + C_m \exp[M(1 - \upsilon\rho)\omega^2(r^2 - r_m^2)/2RT] \quad (1)$$

where C_r is the concentration of the sample at a particular radial position, C_m is the concentration of the sample at the meniscus, M is the molecular weight, υ is the partial specific volume, ρ is the solvent density, ω is the angular velocity, r is the radial position in centimeters from the center of rotation, r_m is the distance in centimeters from the center of rotation to the meniscus, R is the gas constant, T is the absolute (Kelvin) temperature, and B is a correction term for a nonzero baseline.

Preparation of Anti-NDP-Kinase Antibodies and Immunogold Labeling of Bovine Retina. Rabbits were injected intradermally with 0.05 mg of purified NDP-kinase/animal in Freunds complete adjuvant followed by three 0.05 mg booster injections at 14 day intervals. Animals were bled 1

[2] Certain commercial materials, instruments, and equipment are identified in this manuscript in order to specify the experimental procedure as completely as possible. In no case does such identification imply a recommendation or endorsement by the National Institute of Standards and Technology nor does it imply that the materials, instruments, or equipment identified is necessarily the best available for the purpose.

week after the last booster injection and the sera obtained was used for antibody purification by $(NH_4)_2SO_4$ precipitation and gel filtration.

Bovine retinas were fixed with 4% paraformaldehyde and 0.5% glutaraldehyde in 100 mM sodium cacodylate, pH 7.4. After an overnight incubation, the fixed retina were washed in 100 mM sodium cacodylate, pH 7.4, and then dehydrated for 15−20 min at 4 °C in an ethanol gradient composed of 25, 40, 50, 60, 70, 80, and 90% (v/v) ethanol and then three times in 100% ethanol. The specimens were transferred into a mixture of LR Gold Resin:100% ethanol (1:1) for 2−4 h and then into pure LR Gold Resin for an additional 1−2 h at 4 °C. Infiltration in LR Gold Resin was performed at 4−6 °C overnight. Resin-filled polyethylene capsules were held in a rack made of wire and placed in a box coated with aluminum foil on the inside and polymerization was carried out with a UV light source ($\lambda_{max} = 360$ nm) at 12−14 °C. Thin sections (70−90 nm) were cut with an LKB ultrotome using glass knives. All subsequent incubation steps were performed at 4 °C. Nonspecific background staining was blocked with 0.1% ovalbumin in phosphate-buffered saline (PBS), pH 7.4, containing 0.02% NaN_3 for 4 h. Sections were incubated with the anti-NDP-kinase antibodies for 3−4 days, washed with PBS three times for 15−20 min, and then incubated with protein A-10 mm Colloidal Gold (diluted 1:20 in PBS) for 1−2 days. As a control, sections were also incubated with preimmune serum and similarly processed. Immunogold labeled sections were washed with distilled water, stained in 70% ethanol saturated with uranyl acetate and lead citrate in routine fashion, and examined with a JEM 100B electron microscope. Magnifications were calibrated by using cross-grating replicas ($d = 0.463$ μm).

Carbohydrate Analysis. The purified NDP-kinase subunits were separated by SDS−PAGE, electroblotted onto poly(vinyldifluoride) membranes, stained with Ponceau S, and the individual polypeptides excised with a razor blade. The strips were destained, washed extensively with deionized water, and dried. Acid hydrolysis of oligosaccharides in the separated NDP-kinase polypeptides was performed essentially as described (*24*). The oligosaccharides were coupled with 7-amino-4-methylcoumarin (*25*), and the monosaccharide fluorescent derivatives separated on an Ultrasphere ODS column (22 × 0.21 cm) with a mobile phase consisting of 6.8% 2-propanol, 3.5% acetonitrile, and 0.01% trifluoroacetic acid at a flow rate of 0.2 mL/min.

Isolation and Sequence Determination of Peptides Derived from NDP-Kinase. Purified NDP-kinase (1 mg) was heat denatured in 100 mM $NaHCO_3$, pH 9.0, at 95 °C for 10 min and subjected to trypsin digestion (1:50, trypsin:NDP-kinase) at 37 °C for 6 h. The digest was applied to a reverse phase HPLC Zorbax C18 column (25 × 0.5 cm) and eluted with a linear gradient of 0 to 70% acetonitrile containing 0.1% trifluoroacetic acid. Several peak fractions were collected and further purified on the same column. The peptides were sequenced by Edman degradation on a liquid-phase sequencer (Applied Biosystems model 475A).

Screening of the Bovine Retinal cDNA Library. Two oligonucleotides based on the sequences of the tryptic peptides, as well as two additional probes corresponding to the most conserved sequences of NDP-kinases from different sources, were synthesized on an Applied Biosystems model 381A synthesizer. The oligonucleotide probes were 5′-end labeled with ^{32}P using T4 polynucleotide kinase as described (*26*). A bovine retinal cDNA library in bacteriophage λ-ZAP (provided by M. Applebury, Massachusetts Eye and Ear Infirmary) was used for the screening. To screen the library, 4×10^6 bacteriophage was plated out, and filter replicas were prepared using Hybond nitrocellulose filters. The hybridization protocol was adapted from ref *26* with slight modifications to our system. Briefly, the procedure was carried out in the minimal volume of the hybridization buffer with addition of purified radioactively labeled oligonucleotide probe for 1 h at 67 °C and then incubated overnight with slow cooling and shaking. The filters were washed in 4× SSC solution containing 0.1% SDS. Autoradiography was performed using Hyperfilm-βmax film with an intensifying screen for 48 h at −70 °C. Isolation of phage DNA and subcloning of cDNA inserts in the pBluescript M13 vector were done as descibed (*27*). The plasmids were amplified in *Escherichia coli* strain XL-1 Blue, the DNA was purified, and the inserts were sequenced using the dideoxy chain-termination method of DNA sequencing (*28*). Two distinct cDNA clones, designated NBR-A and NBR-B, were isolated and characterized.[3]

Expression and Purification of NBR-A and NBR-B NDP-Kinases. The cDNAs were ligated into the vector pALTER-*Ex*2 at the unique *Eco*RI restriction site in the multiple cloning region. Proper insertion and orientation of NBR-A and NBR-B in the vector were confirmed by restriction enzyme analysis. The *E. coli* strain JM109 (DE3) was transformed with the vector pALTER-Ex2 harboring the NBR-A and NBR-B cDNAs. The transformation mixtures were spread on LB/agar plates containing tetracycline, and after 16−18 h at 37 °C, colonies were isolated and cultured overnight at 37 °C in LB broth containing tetracycline. The overnight cultures were used to inoculate 500 mL of LB broth containing tetracycline in a 1 L capacity shake flask. After further growth at 37 °C for 16 h, the cells were harvested by centrifugation, disrupted in a French pressure cell, and purified by $(NH_4)_2SO_4$ precipitation and chromatography on Blue Sepharose essentially as described above.

Electrophoretic Analysis of NDP-Kinase. Protein samples were analyzed by SDS−PAGE (*29*) with a 5% stacking and a 15 or 16% resolving gel. The proteins were visualized by staining with Coomassie Blue or transferred to poly(vinyldifluoride) membranes (*30*) for immunoblot analysis. Immunoreactive protein was detected using the anti-NDP-kinase primary antibody and horseradish peroxidase conjugated goat anti-rabbit IgG as the second antibody. The protein bands were visualized by chemiluminescence. Isoelectric focusing of NDP-kinase was performed using the Pharmacia Multiphor II IEF system using 5% polyacrylamide slab gels containing 2% Pharmalyte and 10% glycerol (pH range 5.5−8.5).

Crystallization of NBR-A and NBR-B. Crystallization conditions for the two proteins were screened using Hampton Crystallization Kits I and II. The hanging drop vapor diffusion method was used at room temperature for all of the crystallizations. The 10 μL crystallization drops were formed by combining equal volumes of protein solution and

[3] The novel nucleotide sequence data reported here has been deposited with the EMBL Sequence Data Bank and is available under accession number X92956 for NBR-A and X92957 for NBR-B.

reservoir solution. For NBR-A, the final reservoir contained 100 mM sodium acetate, pH 5.0, 200 mM ammonium acetate, and 15% 4K poly(ethylene glycol). The final drop also contained 5 mM cGMP. The crystals were long rods that appeared in 2 days and grew to 0.1 × 0.2 × 0.8 mm in 3 days. If not used immediately, the crystals redissolved within 8 days. The final crystallization reservoir solution for NBR-B contained 100 mM Tris-HCl, pH 7.0, and 2.3 M $(NH_4)_2SO_4$. The final drop also contained 2.5 mM cGMP. The crystals were large bipyramids that grew to 0.7 × 0.6 × 0.6 mm in 5 months. In contrast to NBR-A, the NBR-B crystals showed no degradation with time.

X-ray Data Collection. Diffraction data were collected using Cu Kα X-rays generated by a Siemens rotating anode source operated at 40 kV and 80 mA with a 0.3 mm collimator. A Siemens Hi-Star electronic area detector was positioned 140 mm from the crystal, and at a 2θ angle of 20° for NBR-A and at 150 mm and at a 2θ angle of 20° for NBR-B. The crystals were frozen in nylon loops in cryosolutions made from reservoir solutions containing 20% glycerol for NBR-A and containing 10% 8 K PEG for NBR-B. The high-salt NBR-B crystals dissolved when glycerol was used as a cryoprotectant. During data collection, the crystals were maintained at 100 K by an Oxford Cryosystem coldstream. Diffraction data were processed with Xengen (*31*).

Structure Solution. The structures were solved by molecular replacement using the AmoRe program (*32*) from the CCP4 package (*33*). A combination of the refinement programs XPLOR (*34*) and TNT (*35*) was used to refine the atomic positions and thermal factors. The atomic coordinates and structure factors for NBR-A and NBR-B have been deposited with the Protein Data Bank (*36*).[4]

Other Assays. Protein determinations were done using the BCA method with bovine serum albumin as the standard.

RESULTS

Purification and Properties of Bovine Retinal NDP-Kinase. Bovine retinal NDP-kinase was purified by one successive chromatography step on Blue Sepharose after two steps of ammonium sulfate precipitation. The yield of purified enzyme was ~1 mg from 200 retina, and the specific activity was ~763 units/mg. No appreciable difference was observed in the yield of NDP-kinase or in its functional properties after purification was performed from light- or dark-adapted retina. Purified NDP-kinase was found to be free of guanylate kinase and adenylate kinase activities.

NDP-kinase exhibited a doublet on SDS−PAGE, with the molecular masses of the two polypeptides estimated to be ~17.5 and 18.5 kDa (Figure 1A, lane 1). Both of these polypeptides were barely visible in the crude retinal extract or in the pellet obtained after 75% saturation with $(NH_4)_2SO_4$, further emphasizing their relatively low abundance compared to other soluble retinal proteins. Immunoblot analysis of the purified enzyme using anti-NDP-kinase polyclonal antibodies also showed the two polypeptides (Figure 1B, lane 1). The isoelectric focusing pattern of NDP-kinase shows seven to eight protein bands with a pI range from 7.4 to 8.2 (data not shown). Such a plurality of protein bands could be explained by the existence of NDP-kinase oligomers composed of different proportions of the constitutive subunits and/or by varying degrees of phosphorylation within these oligomers. Sedimentation equilibrium of NDP-kinase (Figure 2) yielded a single, homogeneous species with a molecular mass of 96 ± 2 kDa. This molecular mass closely approaches that of a hexamer, which is characteristic of virtually all eukaryotic NDP-kinases (*37*−*43*).

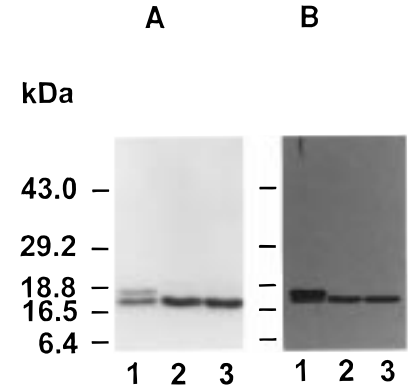

FIGURE 1: Electrophoretic analysis of retinal and recombinant NDP-kinases. (A) Coomassie blue stain of purified bovine retinal NDP-kinase (lane 1), purified NBR-A (lane 2), and purified NBR-B (lane 3) separated by SDS−PAGE. (B) immunoblot analysis of purified bovine retinal NDP-kinase (lane 1), purified NBR-A (lane 2), and purified NBR-B (lane 3) separated by SDS−PAGE. The polypeptides were detected with the polyclonal anti-NDP-kinase antibodies, and visualized by chemiluminescence. Positions of molecular size standards are shown on the left.

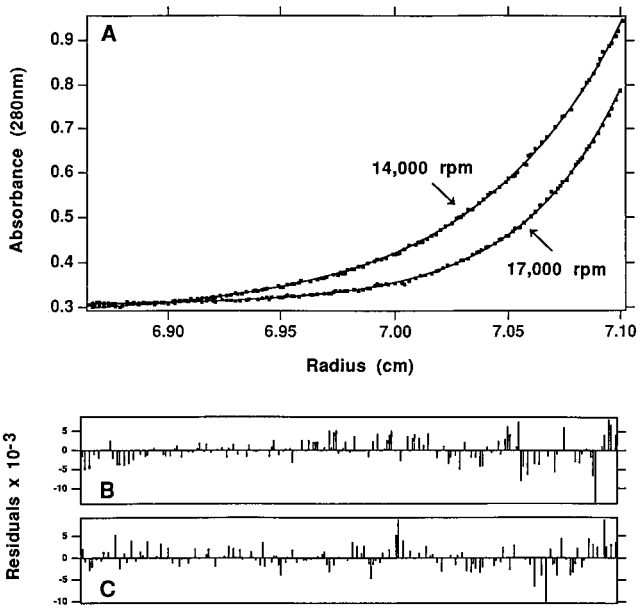

FIGURE 2: Sedimentation equilibrium of retinal NDP-kinase. Sedimentation equilibrium was performed in TMED buffer. (A) Representative traces of absorbance at 280 nm versus radial distance in centimeters at 14 000 and 17 000 rpm. (B and C) the residuals ($A_{theoretical} - A_{observed}$) for a single species of molecular mass 96 000 Da at 14 000 and 17 000 rpm, respectively. Sedimentation equilibrium of NBR-A and NBR-B NDP-kinases showed similar results and yielded an absolute molecular mass of 97 000 and 95 000 Da, respectively.

Functional Properties of Retinal NDP-Kinase. The K_m values for NDP-kinase were determined at fixed and varying concentrations of diphosphate and triphosphate nucleotides (Table 1). Like other NDP-kinases, retinal NDP-kinase also

[4] The atomic coordinates and structure factors reported here have been deposited with the Protein Data Bank and are available under accession nos. 1BHN for NBR-A and 1BE4 for NBR-B.

Table 1: K_m Values for NDP-Kinase in the Presence of Various Nucleoside Diphosphate and Triphosphate Substrates

substrate	K_m (mM)[a]
ATP	0.104
GTP	0.327
CDP	1.160
TDP	1.290

[a] The K_m values were determined from by the Florini−Vestling method (*23*).

Table 2: Monosaccharide Content of NDP-Kinase Subunits

	carbohydrate content[a]		
monosaccharides	(μg)	(pmol)	% total carbohydrate[a]
Gal	0.11	611	30.6
Man	0.09	500	25.0
GlcNAc	0.12	542	33.3
Fuc	0.01	61	2.8
GalNAc	0.03	135	8.3

[a] For carbohydrate analysis, 30 μg of each NDP-kinase polypeptide was used. The results shown are for the 17.5 kDa polypeptide. Virtually identical results were found for the 18.5 kDa polypeptide.

shows broad specificity for the nucleotide substrate. The K_m of the enzyme for ATP (104 μM) was the lowest among the nucleotides tested, while that for GTP was only about three times higher. Because of this relatively small difference in the K_m values, it was not possible to obtain accurate and reproducible kinetic measurements using ATP and GDP as the donor and acceptor substrates, respectively.

Carbohydrate Analysis of Retinal NDP-Kinase. Given the rather small difference in apparent molecular mass between the two NDP-kinase polypeptides (∼1 kDa), we surmised that this may be the result of some posttranslational modification. The results of carbohydrate analysis on the 17.5 kDa NDP-kinase polypeptide are shown in Table 2. Virtually identical results were obtained for the 18.5 kDa polypeptide. Both contained equivalent amounts of Gal, Man, GlcNac, Fuc, and GalNac saccharides, which are characteristic of O-linked glycosylation. The total content of carbohydrate in each polypeptide accounts for 2−3% of protein weight. Consequently, retinal NDP-kinase can be referred to as a glycoprotein with a low content of oligosaccharides. Although it is possible that some properties of this enzyme could be explained by the presence of carbohydrates, it is evident that the difference in molecular mass of the NDP-kinase subunits may not be attributed to a distinction in oligosaccharide content.

Subcellular Localization of NDP-Kinase in Bovine Retina. Figure 3 shows an electron micrograph of immunogold-labeled bovine retinal sections that had been first incubated with polyclonal anti-NDP-kinase antibodies. The gold particles were primarily localized along the rod outer segment (ROS) disk membranes, but some of the particles were found on the plasma membrane and in the cytoplasm as well. From these results, it seems reasonable to conclude that ROS NDP-kinase may exist in both membrane-associated and cytosolic forms.

Cloning of Bovine Retinal NDP-Kinase. Direct sequence analysis of NDP-kinase did not show cleavage of any amino acids, suggesting that the NH_2-terminal residue in each of the polypeptides is blocked. The nature of this blocking group remains to be determined. Digestion of NDP-kinase with trypsin after heat denaturation at elevated pH allowed exhaustive cleavage of the protein and provided facile peptide purification and sequencing. Using this sequence information and taking into account the codon usage of several known retinal proteins, two oligonucleotides were synthesized and used to screen a bovine retinal cDNA library. Two additional probes, constructed on the basis of the most conserved amino acid sequences of known NDP-kinases, were used as controls.

Initial screening of the bovine retinal cDNA library yielded several positive clones and, among them, one containing the whole sequence of NDP-kinase (subsequently termed NBR-A). Taking into consideration the occurrence of at least two NDP-kinase isoforms in other eukaryotic cells, a second round of screening was attempted using four unique probes based on the nucleotide sequence of the full-length retinal NDP-kinase cDNA (NBR-A). This second round of screening yielded another clone, termed NBR-B (they are designated as A and B in analogy with NDP-kinases from other sources). The clone containing NBR-A had a 696 bp long insert while that containing NBR-B had an 863 bp insert.

Sequence analysis of NBR-A and NBR-B showed considerable base differences in both the 5′- and 3′-noncoding regions, suggesting that they are indeed isoforms of the enzyme. Further, NBR-A and NBR-B differ from each other in four codons. Two nucleotide substitutions are responsible for the amino acid diversity of the NDP-kinase isoforms: Ile-21 and Arg-135 in NBR-A are replaced by Met and His residues, respectively, in NBR-B (Figure 4). The other two codon changes (at Pro-72 and Gly-106) do not result in amino acid substitutions. The deduced amino acid sequences of the NDP-kinase isoforms each consist of 152 residues and the calculated molecular masses are 17 262 kDa for NBR-A and 17 299 kDa for NBR-B.

Purification and Properties of Expressed NBR-A and NBR-B. The purification protocol for retinal NDP-kinase was successfully adapted for the preparation of NBR-A and NBR-B expressed in *E. coli*. The yields of purified NBR-A and NBR-B were typically 18−20 mg from a 500 mL shake flask culture, and the specific activities were ∼857 units/mg and ∼1063 units/mg, respectively. Similar to retinal NDP-kinase, the K_m of the expressed enzymes for ATP was the lowest among the nucleotides tested with GTP showing a 3-fold higher difference.

NBR-A and NBR-B each showed a single polypeptide chain of ∼17 kDa on SDS−PAGE (Figure 1, lanes 2 and 3, respectively). Immunoblot analysis of the expressed enzymes using anti-NDP-kinase polyclonal antibodies raised against the retinal enzyme also showed only the 17 kDa polypeptide (Figure 1B, lanes 2 and 3). Similar to retinal NDP-kinase, the isoelectric focusing patterns of NBR-A and NBR-B show six to seven major protein bands. However, the pI range for NBR-A was 8.0−8.5 while that for NBR-B was 6.5−7.5. Sedimentation equilibrium of the NBR-A and NBR-B isoforms showed molecular masses of 97 and 95 kDa, respectively (data not shown). Like retinal NDP-kinase, this is suggestive of a hexameric arrangement for the expressed enzymes.

Overall Structure of NBR-A and NBR-B NDP-Kinases. NBR-A and NBR-B were subjected to crystallographic analysis in the presence of cGMP, a putative competitive

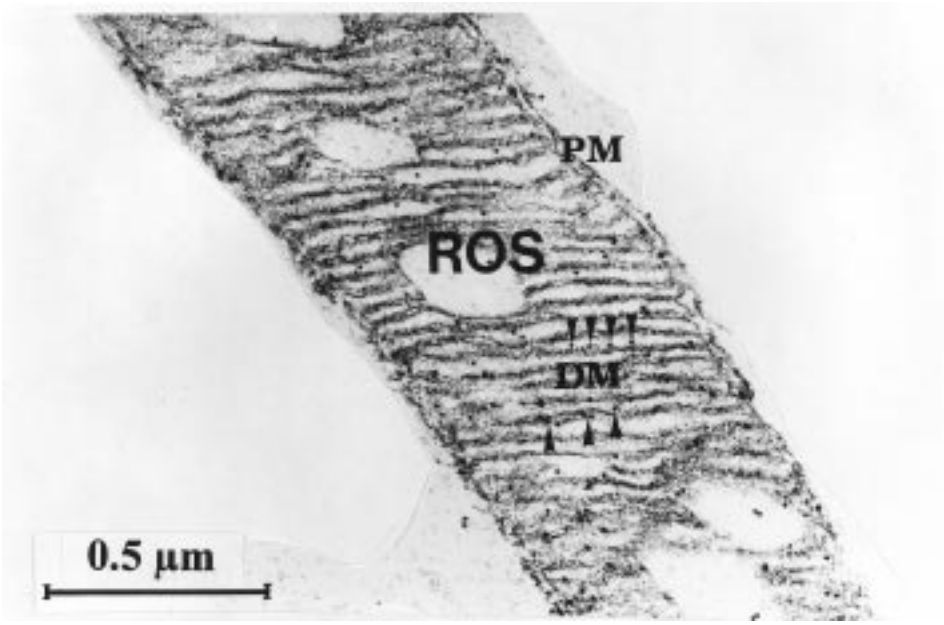

FIGURE 3: Transmission electron micrograph of a longitudinal section of bovine retina indirectly labeled for NDP-kinase via the immunogold method. The retina were prepared and labeled as described in the Materials and Methods using polyclonal anti-NDP-kinase antibodies and protein A-colloidal gold. The gold particles are evident along the ROS disk membranes (DM), the plasma membrane (PM), and in the cytoplasm close to the RIS. Arrowheads show gold particles localized along the DM. The bar represents 0.5 μm.

inhibitor of retinal NDP-kinase, and their 2.4 Å resolution structures were determined by molecular replacement. The X-ray data and refinement statistics for NBR-A and NBR-B are shown in Table 3. The three-dimensional structures of NBR-A and NBR-B are very similar to each other and to the structures of NDP-kinases from other sources (*8, 10*−*12*). The monomer folds into a compact structure with a four-stranded antiparallel β-sheet partially covered by α-helices (Figure 5). The amino acid residues 53−58 form a boundary for the nucleotide-binding pocket. The region that includes amino acid residues 93−115 is labeled the Kpn loop in reference to a *Drosophila* mutant. The sequence of this region is strictly conserved between the bovine retinal and *Drosophila* NDP-kinases and is involved in the most significant trimer contacts. The carboxyl-terminal residue Glu-152 defines the edge of the nucleotide pocket of its neighbor in the trimer. Orthogonal stereoviews of the NBR-A hexamer with each subunit colored differently emphasize this point (Figure 6).

Nucleotide-Binding Site. The nucleotide-binding site of NBR-A and NBR-B are very similar to those described for other NDP-kinases (*8, 10*−*12*). A stereoview of the NBR-B active site with bound cGMP is shown in Figure 7. The guanosine base of cGMP is stacked face-to-face with Phe-160 and Val-112 is on the opposite side. Both of these residues are conserved across species with only one exception. In *Myxococcus xanthus*, the position equivalent to 112 is an Ile (Figure 4). Notably, the active site of NBR-A contained both a cGMP and a GDP molecule bound at half occupancy. Both nucleotides interact similarly with the active-site residues of the enzyme.

DISCUSSION

To understand the biochemical events controlling the synthesis of guanine nucleotides involved in visual transduction, the isolation and characterization of retinal enzymes involved in nucleotide metabolism are desirable. In this paper, a study was undertaken to purify, biochemically characterize, clone, and crystallize one of the key enzymes supporting high levels of GTP in vertebrate photoreceptor cells: NDP-kinase.

Bovine retinal NDP-kinase, like those from other sources (*37*−*39*), shows two distinct protein bands with apparent molecular masses of 17.5 and 18.5 kDa when analyzed by SDS−PAGE (Figure 1). In contrast, both NBR-A and NBR-B showed a single polypeptide chain of ∼17 kDa. It is interesting that the correspondence between separate polypeptides and the products of gene isoforms was determined only for human erythrocyte NDP-kinase (*40*). By protein sequencing, it was shown that the human NDP-kinase-A (upper protein band on SDS−PAGE) and NDP-kinase-B (lower protein band on SDS−PAGE) polypeptide chains are identical to Nm23-H1 and Nm23-H2, respectively, the amino acid sequences of which were deduced from the nucleotide sequences of the corresponding genes (*41, 42*). Both the SDS−PAGE and cDNA cloning results indicate that there exists at least two NDP-kinase isoforms in bovine retina (Figures 1 and 4), as is the case for other higher eukaryotes (*42*−*44*). However, NBR-A and NBR-B are remarkably similar in their coding nucleotide and amino acid sequences with identities of 99.1 and 98.8%, respectively. Therefore, the ∼1 kDa difference in apparent molecular weight between the two retinal NDP-kinase polypeptides suggests that either they are subject to different posttranslational modifications or bovine retina contain yet another NDP-kinase isoform.

Sedimentation equilibrium of the retinal (Figure 2) and expressed NDP-kinases suggests that the enzymes exist as a hexamer. This is further substantiated by the three-dimensional structures of NBR-A and NBR-B (Figure 6). Tetrameric structure is inherent in bacterial NDP-kinases from *M. xanthus* and *E. coli*, and such a subunit structure is

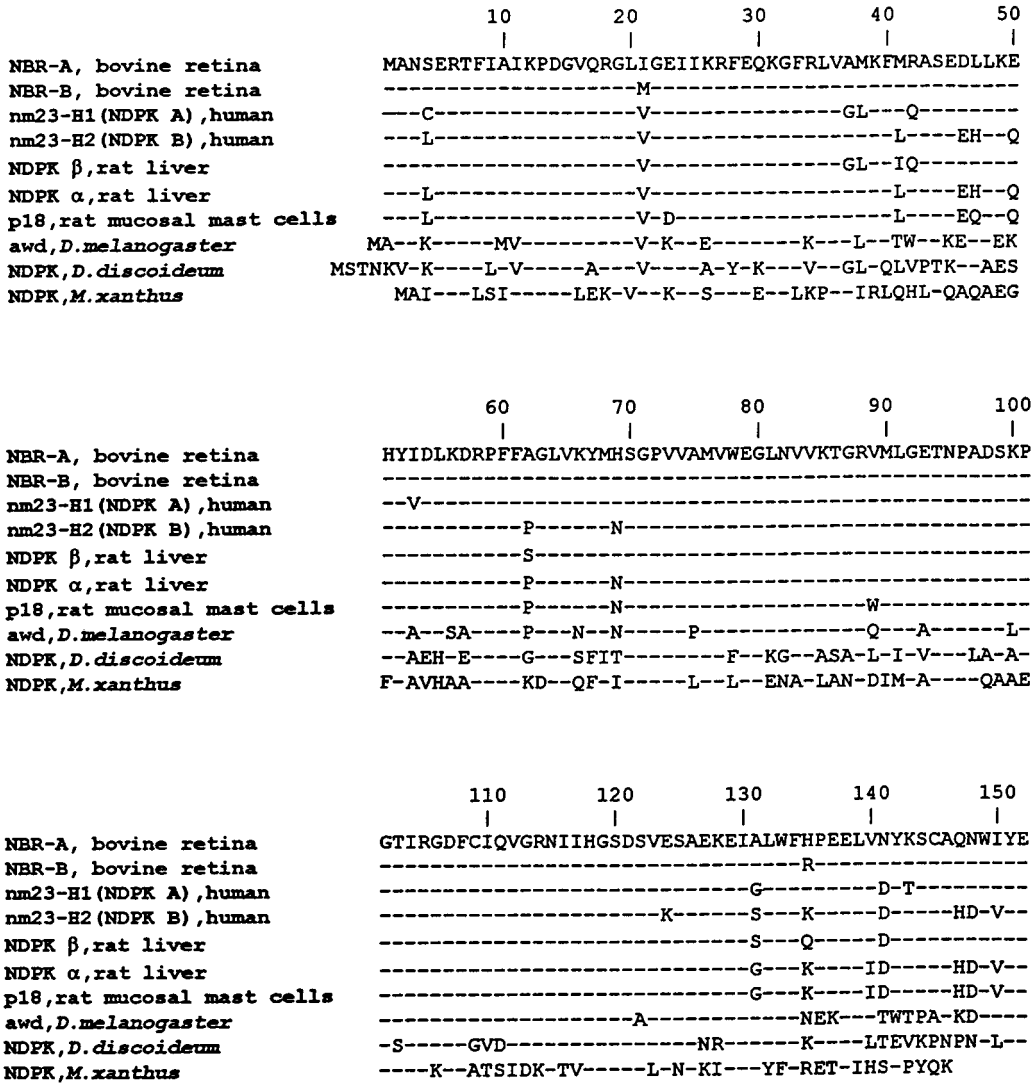

FIGURE 4: Comparison of retinal NDP-kinase with NDP-kinases from other sources. The deduced amino acid sequences of NBR-A and NBR-B were compared with those of human nm23-H1 (*41*), human nm23-H2 (*42*), rat liver NDP-kinase α (*60*), rat liver NDP-kinase *β* (*43*), rat mucosal mast cell p18 (*66*), *D. melanogaster awd* (*41*), *D. discoideum* NDP-kinase (*67*), and *M. xanthus* NDP-kinase (*68*).

Table 3: Data and Refinement Statistics[a]

	NBR-a	NBR-b
space group	$P2_12_12_1$	$P4_32_12$
cell parameters (*a*,*b*,*c*) (Å)	89.88, 92.11, 131.63	128.62, 128.62, 88.18
content of asymmetric unit	hexamer	trimer
resolution limit of data (Å)	2.4	2.4
unique reflections	41 872	30 274
R_{sym}	12.2	10.9
refinement		
R-factor	0.200	0.198
no. of waters	310	282
geometry—rms deviation		
bond length (Å)	0.021	0.024
bond angles (deg)	5.13	5.53

[a] A more complete set of data and refinement statistics as well as a detailed description and comparison of the NBR-A and NBR-B structures will be published elsewhere.

not common for proteins from eukaryotic organisms where the hexameric form is most frequent (*8*, *9*, *45*−*52*).

Posttranslational modifications of retinal NDP-kinase appear to include glycosylation, blocking of the NH_2-terminal amino acid, and most probably, phosphorylation. Both subunits of the enzyme from bovine retina contain ∼2−3% (w/w) of carbohydrate, which consists of Gal, Man, GlcNac, Fuc, and GalNac saccharides (Table 2). All eukaryotic NDP-kinases contain a potential O-glycosylation site [ERTF (*53*), amino acid residues 5−8], and another consensus O-glycosylation motif, VKTG (amino acid residues 84−87), is preserved in proteins from mammals and *D. melanogaster* (Figure 4). These potential glycosylation sites are also on the outside of the molecule and readily accessible for modification (Figure 5). In fact, these sites are adjacent to one another; the distance between the C_α of Glu-5 and Val-84 is 7 Å. The assumption of NH_2-terminal amino acid blocking is inferred from the absence of Edman degradation on retinal NDP-kinase. Although the NH_2-terminal Met is not included on the structures reported here, Ala-2 is on the surface of the molecule (Figure 5). Differences in the extent of amino acid residue phosphorylation were implied from the isoelectric focusing experiments on both the retinal and expressed enzymes. The His-118 residue, a phosphorylation site on NDP-kinase, is present in all known NDP-kinases (Figure 4). NBR-A and NBR-B both contain an AMKF sequence (amino acid residues 37−40) which is nearly conserved as the ATP-binding region in cyclic nucleotide-dependent protein kinases. Lys-39 in this region is invariant

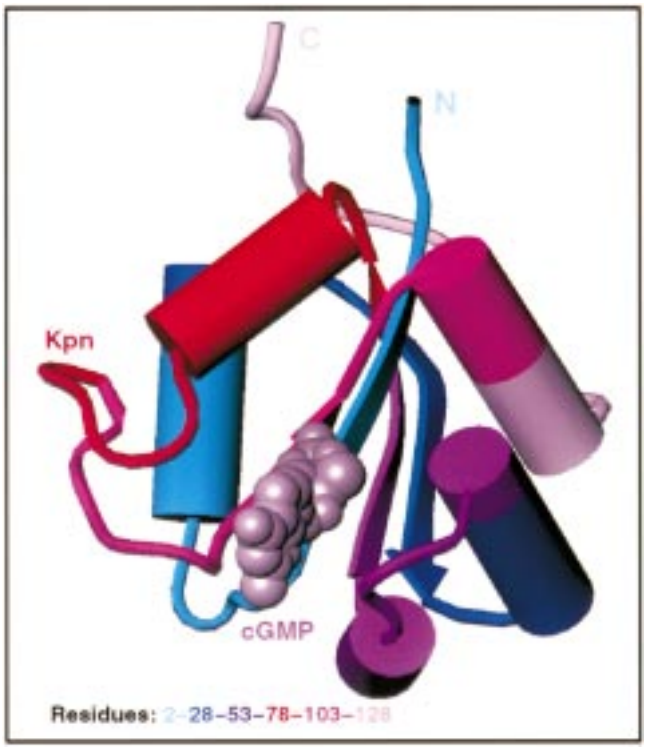

FIGURE 5: The fold of an NBR-B monomer. The α-helices are represented by cylinders and the β-sheets by ribbons. The colors represent the sequence which goes from light blue for the amino-terminus to light pink for the carboxyl-terminus. The loop region designated as "Kpn" is labeled, and a space filling model of cGMP is shown in the active site.

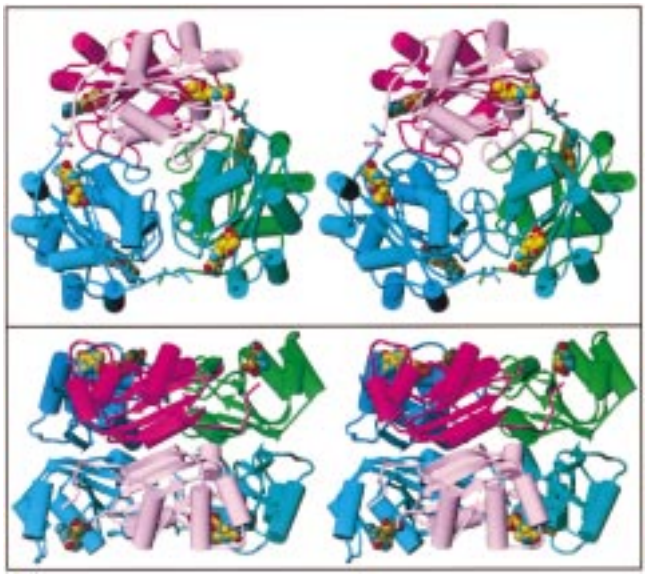

FIGURE 6: Orthogonal stereoviews of an NBR-A hexamer. Each monomer (A−E) of the hexamer is shown in a different color. The α-helices are represented by cylinders and the β-sheets by ribbons. The protein is shown with its secondary structure and the nucleotides, cGMP, are represented as space filling models.

in nearly all NDP-kinases and is essential for catalytic activity (*60*).

Kinetic studies of retinal and expressed NDP-kinases showed that the enzymes display low substrate specificity (Table 2), as illustrated for other NDP-kinases. However, NDP-kinase can function in a low ATP containing enviroment (K_m of retinal NDP-kinase for ATP of ∼104 μM) with high velocity, supplying a sufficient level of nucleoside triphosphates in visual cells. The specific activity of retinal NDP-kinase, ∼763 units/mg, is considerably high when compared with other guanine nucleotide pathway enzymes. For example, the specific activity of retinal guanylate kinase is ∼340 units/mg (*5*). The turnover number of NDP-kinase is 229 mol of CTP produced/mol of enzyme/s or 1374 mol of CTP produced/mol of enzyme/s for a hexamer. This is considerably greater than the turnover number of guanylate kinase (∼130 mol of GDP produced/mol of enzyme/s). These findings suggest that even relatively small amounts of guanylate kinase (*20, 54*) and NDP-kinase in the ROS are greater in terms of absolute activity than guanylate cyclase (*55*−*58*). Therefore, these two enzymes may support local cGMP requirements at the expense of ATP, which is produced abundantly in the ROS as a result of anaerobic glycolysis (*59*), without the need for shuttling GMP from the ROS to the rod inner segment (RIS) for conversion to GTP.

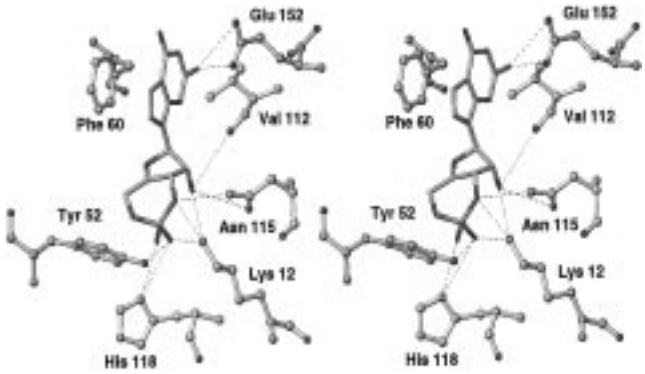

FIGURE 7: Stereoview of the active site with cGMP. The active site of NBR-B chain C with bound cGMP is shown in stereo. The polar contacts are represented with dashed lines. All of the residues shown are from chain C except for Glu-152, which is the terminal residue in chain A.

The specific activities of purified NBR-A and NBR-B, 857 units/mg and 1063 units/mg, respectively, are slightly higher than the retinal enzyme. This difference in specific activity between the two isoforms is most likely due to the amino acid variance at position 135, which is a His in NBR-A and an Arg in NBR-B (Figure 4). Residue 135 is on the exterior of the molecule near the 2-fold interface (Figures 5 and 6). It is also possible that this charge difference may influence the phosphorylation state of the protein and account for the observed differences in pI between the two isoforms. Since the exact amino acid composition or polypeptide composition of the retinal NDP-kinase hexamer is not known, it is difficult to rationalize the observed difference in specific activity and pI from the NBR-A and NBR-B isoforms.

The enzyme pattern of NDP-kinase has been localized almost exclusively to the RIS (*4*), a region of the rod cell that contains the biosynthetic and bioenergetic pathways. However, NDP-kinase with the same kinetic and electrophoretic properties can be isolated from highly purified ROS,[5] suggesting that the enzyme is compartmentalized in both the ROS and RIS. These observations are consistent with our immunocytochemical electron microscopy data (Figure 3), which shows the distribution of NDP-kinase in the ROS.

[5] N.G.A., unpublished observations.

Interest in the possible role of NDP-kinase in a variety of signal transduction pathways has dramatically increased, and much evidence exists for participation of the enzyme in this process. It was shown that plasma membrane bound NDP-kinase may function as a GTP supply machinery for the G-protein involved in hormone-dependent adenylate cyclase systems (*61*). NDP-kinase can transfer the γ-phosphate of ATP directly to GDP bound to G proteins, and this phosphorylation results in the activation of the signal-coupling proteins (*62*). One possible way in which NDP-kinase participates in signal transduction was proposed by Ruggieri and McCormick (*63*). Although the GTP level in the cell is estimated to be much higher than that of GDP, a local GTP:GDP ratio may have a significant impact on the nucleotide supply in the immediate vicinity of the G-protein. This ratio is altered as a result of NDP-kinase activity. Existence of such GTP and GDP microcompartments could account for effect of NDP-kinase on G-proteins. Further, since cGMP levels in the retina are directly influenced by GTP via guanylate cyclase, it is reasonable to consider that cGMP itself may act as a competitive inhibitor of NDP-kinase in order to prevent the further conversion of GDP to GTP. In NDP-kinase from *M. xanthus*, cAMP is known to act as a competitive inhibitor of the enzyme (*64*). Similar effects of cAMP and various cAMP analogues on the ATP/GDP phosphotransferase activity of Nm-23 have also been reported (*65*). The active sites of NBR-A and NBR-B can accommodate a GDP and/or a cGMP molecule (Figures 5 and 7), suggesting that cGMP may serve to inhibit the phosphotransferase activity of retinal NDP kinase. Like NBR-A and NBR-B, the active site of the *M. xanthus* NDP-kinase/cAMP closely resembles that of the ADP-ligated complex (*64*).

The biochemical and structural characterization of NDP-kinase from bovine retina will allow us to further investigate its role in the regulation of the GTP supply to G-proteins and other components involved in visual transduction. The availability of the cDNA sequences for retinal NDP-kinase should allow for the overexpression of mutant forms of the enzyme in sufficient quantities for three-dimensional structure determination.

ACKNOWLEDGMENT

We would like to thank N. S. Bystrov for oligonucleotide synthesis, O. M. Hodova for carbohydrate analysis, and N. N. Sykilinda for assistance in preparation of the polyclonal antibodies. We are also indebted to S. S. J. Lee for technical assistance, T. Ngo for assistance in preparing the manuscript, J. Zondlo for GroES, and R. Molday for the rho 1D4 antibody.

REFERENCES

1. Chabre, M., and Deterre, P. (1989) *Eur. J. Biochem. 179*, 255−266.
2. Lagnado, L., and Baylor, D. (1992) *Neuron 8*, 995−1002.
3. Stryer, L. (1991) *J. Biol. Chem. 266*, 10711−10714.
4. Berger, S. J., DeVries, G. W., Carter, J. G., Schulz, D. W., Passonneau, P. N., Lowry, O. H., and Ferrendelli, J. A. (1980) *J. Biol. Chem. 255*, 3128−3133.
5. Hall, S. W., and Kuhn, H. (1986) *Eur. J. Biochem. 161*, 551−556.
6. Agarwal, R. P., Robison, B., and Parks, R. E., Jr. (1978) *Methods Enzymol. 51*, 376−386.
7. DeLaRosa A., Williams, R. L., and Steeg, P. S. (1995) *BioEssays 17*, 53−62.
8. Dumas, C., Lascu, I., Morera, S., Glaser, P., Fourme, R., Wallet, V., Lacombe, M. L., Veron, M., and Janin, J. (1992) *EMBO J. 11*, 3203−3208.
9. Williams, R. L., Oren, D. A., Dorado, J. M., Inouye, S., Inouye, M., and Arnold, E. (1993) *J. Mol. Biol. 234*, 1230−1247.
10. Morera, S., LeBras, G., Lascu, I., Lacombe, M. L., Veron, M., and Janin, J. (1994) *J. Mol. Biol. 243*, 873−890.
11. Webb, P. A., Perisic, O., Mendola, C. E., Backer, J. M., and Williams, R. L. (1995) *J. Mol. Biol. 251*, 574−587.
12. Xu, Y.-W., Morera, S., Janin, J., and Cherfils, J. (1997) *Proc. Natl. Acad. Sci. U.S.A.* 94, 3579−3583.
13. Deazolf, C. R., Tripoulas, N., Biggs, J., and Shearn, A. (1988) *Dev. Biol. 129*, 169−178.
14. Postel, E. M., Berberich, S. J., Flint, S. J., and Ferrone, C. A. (1993) *Science 261*, 478−480.
15. Okabe-Kado, J., Kosukabe, T., Honma, Y., Hayashi, M., Henzel, W. J., and Hozumi, M. (1992) *Biochem. Biophys. Res. Commun. 182*, 987−994.
16. Venturelli, D., Martinez, R., Melotti, P., Casella, I., Peschle, C., Cucco, C., Spampinato, G., Darzynkiewicz, Z., and Calabretta, B. (1995) *Proc. Natl. Acad. Sci. U.S.A. 92*, 7435−7439.
17. Munoz-Dorado, J., Almaula, N., Inouye, S., and Inouye, M. (1993) *J. Bacteriol. 175*, 1176−1181.
18. Wagner, P. D., and Ngoc-Diep, V. (1995) *J. Biol. Chem. 270*, 21758−21764.
19. Xu, L., Murphy, J., and Otero, A. de S. (1996) *J. Biol. Chem. 271*, 21120−21125.
20. Gaidarov, I. O., Suslov, O. N., and Abdulaev, N. G. (1993) *FEBS Lett. 335*, 81−84.
21. Shmukler, B. E., Zubov, D. V., and Abdulaev, N. G. (1993) *Bioorg. Khim. 19*, 682−685.
22. Parks, R. E., and Agarwal, R. P. (1973) in *The Enzymes* (Boyer, P. D., Ed.) Vol. 8, pp 307−334, Academic Press, NY.
23. Florini, J. R., and Vestling, C. S. (1957) *Biochim. Biophys. Acta 25*, 575−578.
24. Takemoto, H., Hase, S., and Ikenaka, T. (1985) *Anal. Biochem. 145*, 245−250.
25. Khorlin, A. Ya., Shiyan, S. D., Markin, V. A., Nasonov, V. V., and Mirzayanova, M. N. (1986) *Bioorg. Khim. 12*, 1203−1212.
26. Sambrook, J., Fritsch, E. F., and Maniatis, T. (1989) *Molecular Cloning: A Laboratory Manual*, 2nd ed., Cold Spring Harbor Laboratory Press, Plainview, NY.
27. Short, J. M., Sorge, J. A., and Huse, W. D. (1988) *Nucleic Acids Res. 16*, 7583−7600.
28. Sanger, F., Nicklen, S., and Coulson, A. R. (1977) *Proc. Natl. Acad. Sci. U.S.A. 74*, 5463−5467.
29. Laemmli, U.K. (1970) *Nature 227*, 680−685.
30. Matsudaira, P. (1987) *J. Biol. Chem.* 262, 10035−10038.
31. Howard, A., Gilliland, G. L., Finzel, B. C., Poulos, T. L., Ohlendorf, D. H., and Salemme, F. R. (1987) *J. Appl. Crystallogr. 20*, 383−387.
32. Navaza, J. (1994) *Acta Crystallogr., Sect. A 50*, 157−163.
33. Collaborative Computational Project, Number 4 (1994) *Acta Crystallogr., Sect. A 50*, 760−763.
34. Brunger, A. T. (1992) X-Plor, Yale University, New Haven.
35. Tronrud, D., TenEyck, L., and Matthews, B. W. (1987) *Acta Crystallogr., Sect. A 43*, 489−501.
36. Bernstein, F. C., Koetzle, T. F., Williams, G. J. B., Meyer, E. F., Jr., Brice, M. D., Rogers, J. R., Kennard, O., Shimanouchi, T., and Tasumi, M. (1977) *J. Mol. Biol. 112*, 535−542.
37. Presecan, E., Vonica, A., and Lascu, I. (1989) *FEBS Lett. 250*, 629−632.
38. Kimura, N., and Shimada, N. (1988) *J. Biol. Chem. 263*, 4647−4653.
39. Nickerson, J. A., and Well, W. W. (1984) *J. Biol. Chem. 259*, 11297−11304.30. Yue, R. H., Ratliff, R. L., and Kuby, S. A. (1967) *Biochemistry 6*, 2923−2932.
40. Gilles, A.-M., Presecan, E., Vonica, A., and Lascu, I. (1991) *J. Biol. Chem. 266*, 8784−8789.31. Palmieri, R., Yue, R. H.,

Jacobs, H. K., Maland, L., Wu, L., and Kuby, S. A. (1973) *J. Biol. Chem. 248*, 4486−4499.
41. Rosengard, A. M., Krutzsch, H. C., Shearn, A., Biggs, J. R., Barker, E., Margulies, I. M. K., King, C. R., Liotta, L. A., and Steeg, P. S. (1989) *Nature 342*, 177−180.
42. Stahl, J. A., Leone. A., Rosengard, A. M., Porter, L., King, C. R., and Steeg, P. S. (1991) *Cancer Res. 51*, 445−449.
43. Shimada, N., Ishikawa, N., Munakata, Y., Toda, T., Watanabe, K., and Kimura, N. (1993) *J. Biol. Chem. 268*, 2583−2589.
44. Urano, T., Takamiya, K., Furukawa, K., and Shiku, H. (1992) *FEBS Lett. 309*, 358−362.
45. Yue, R. H., Ratliff, R. L., and Kuby, S. A. (1967) *Biochemistry 6* 2923−2932.
46. Palmieri, R., Yue, R. H., Jacobs, H. K., Maland, L., Wu, L., and Kuby, S. A. (1973*) J. Biol. Chem. 248*, 4486-4499.
47. Lascu, I., Chaffotte, A., Limbourg-Bouchon, B., and Veron, M. (1992) *J. Biol. Chem. 267*, 12775−12781.
48. Hamby, C. V., Mendola, C. E., Potla, L., Stafford, G., and Backer, J. M. (1995) *Biochem. Biophys. Res. Commun. 211*, 578−585.
49. Schaertl, S. (1996) *FEBS Lett. 394*, 316−320.
50. Ulloa, R. M., Muschietti, J. P., Veron, M., Torres, H. N., and Tellezinon, M. T. (1995) *Mol. Biochem. Parasitol. 70*, 119−129.
51. Robinson, J. B., Brems, D. N., and Stellwagen, E. (1981) *J. Biol. Chem. 256*, 10769−10773.
52. Almaula, N., Lu, Q., Delgado, J., Belkin, S., and Inouye, M. (1995) *J. Bacteriol. 177*, 2524−2529.
53. Gooley, A. A., Packer, N. H., Pisano, A., Redmond, J. W., Williams, K. L., Jones, A., Loughnan, M., and Alewood, P. F. (1995) in *Techniques in Protein Chemistry VI*, pp 83−90, Academic Press, NY.
54. Gaidarov, I. O., Suslov, O. N., Ovchinnikova, T. V., and Abdualev, N. G. (1994) *Biorg. Khim. 20*, 367−381.
55. Ames, A., Walseth, T. F., Heyman, R. A., Barad, M., Graeff, R. M., and Goldberg, N. D. (1986) *J. Biol. Chem. 261*, 13034−13042.
56. Aparicio, J. G., and Applebury, M. L. (1995) *Protein Expression Purif. 6*, 501−511.
57. Walliman, T., Wegmann, G., Moser, H., Huber, R., and Eppenberger, M. M. (1986)*Proc. Natl. Acad. Sci. U.S.A. 83*, 3816−3819.
58. Dontsov, A. E., Zak, P. P., Ostrovskii, M. A. (1978) *Biochemistry U. S. S. R. 43*, 471−474.
59. Hsu, S.-C., and Molday, R. S. (1991) *J. Biol. Chem. 266*, 21745−21752.
60. Kimura, N., Shimada, N., Nomura, K., and Watanabe, K. (1990) *J. Biol. Chem. 265*, 15744−15749.
61. Kimura, N., and Shimada, N. (1990) *Biochem. Biophys. Res. Commun. 168*, 99−106.
62. Kikkawa, S., Takahashi, K., Takahashi, K.-I., Shimada, N., Ui, M., Kimura, N., and Katada, T. (1990) *J. Biol. Chem. 265*, 21536−21540.
63. Ruggieri, R. and McCormick, F. (1991) *Nature 353*, 390−391.
64. Strelkov, S. V., Perisic, O., Webb, P. A., and Williams, R. L. (1995) *J. Mol. Biol. 249*, 665−674.
65. Anciaux, K., Van Dommelen, K., Willems, R., Roymans, D., and Slegers, H. (1997) *FEBS Lett. 400*, 75−79.
66. Hemmerich, S., Yarden, Y., and Pecht, I. (1992) *Biochemistry 31*, 4574−4579.
67. Lacombe, M. L., Wallet, V., Troll, H., and Veron, M. (1990) *J. Biol. Chem. 265*, 10018−10025.
68. Munoz-Dorado, J., Inouye, M., and Inouye, S. (1990) *J. Biol. Chem. 265*, 2702−2706.

BI980853S